Vol 13 No 12, December 2004
1009-1963/2004/13(12)/2097-08

Chinese Physics

© 2004 Chin. Phys. Soc.
and IOP Publishing Ltd

Bootstrap current fraction scaling for spherical torus plasmas*

Shi Bing-Ren(石秉仁)†

Southwestern Institute of Physics, Chengdu 610041, *China*

(Received 11 March 2004; revised manuscript received 22 June 2004)

Dependence of the bootstrap current fraction of spherical torus plasma on the aspect ratio and the triangular deformation is studied by using a simple equilibrium model, the Solov'ev-type equilibrium. Two bootstrap current models are used: one is the single-ion collisionless regime model, the other is the recently developed arbitrary collisional regime model. It is found that besides the well known favourable effect of the small aspect ratio on the enhancement of the bootstrap current fraction, the triangularity is beneficial for raising the total bootstrap current though it does not change its fraction much.

Keywords: spherical torus, bootstrap current, triangular deformation
PACC: 5255, 5255G

1. Introduction

The spherical torus (ST) is a very promising approach to the realization of an economic fusion reactor in magnetic fusion research. [1−3] It has been experimentally observed or theoretically demonstrated that this configuration can stably confine plasma with a toroidal beta value as high as 50% or even higher, which is almost 10-times higher than that the tokamak plasma can attain, and it has none of the disruption-type instabilities that have been seriously threatening the stable operation of tokamak. However, the engineering issues are somewhat more formidable than those of the standard tokamak approach. One of the issues to be solved is how to produce and maintain a large toroidal current for a long time in this system. Since the bootstrap current was predicted by the neoclassical theory [4,5] and observed in several tokamaks, the steady state reactor operation for either tokamak or ST has largely relied on this kind of current. Much work has been done relevant to different aspects of this issue.[6−11] One of these is how large a fraction of this current can be in the total toroidal current. Based on the neoclassical transport theory analysis, a general scaling should be as follows:[5]

$$f_{\rm bs} = I_{\rm bs}/I_{\rm p} = C_{\rm bs}\sqrt{\varepsilon}\beta_{\rm p}, \tag{1}$$

where $I_{\rm bs}$ is the total bootstrap current, $I_{\rm p}$ the total toroidal plasma current, ε the inverse aspect ratio, $\beta_{\rm p}$ the poloidal plasma beta value, while $C_{\rm bs}$ a function of multi-variables such as plasma density, temperature, current profile, ion charge, collisionality and equilibrium characteristics, respectively. To obtain a more concrete form, a relatively simple scaling is[6]

$$f_{\rm bs} \propto \sqrt{\varepsilon}\frac{a^2\langle p\rangle}{I_{\rm p}^2}\frac{1+\kappa^2}{2}. \tag{2}$$

2. Bootstrap current model

In this paper, we mainly discuss two bootstrap models: the first one is the single-ion collisionless regime model[4] that has been widely used for high temperature tokamak plasmas. The second one is the arbitrary collisional regime model based on the appropriate interpolation of exact but very complicated results in different collisional regimes.[7] Because the bootstrap current can only appear as an averaged parallel current, its general form should be $\langle jB\rangle_{\rm bs}$, where $\langle\ \rangle$ denotes an average over a given magnetic surface. For the first model, this quantity stands[4] at

$$\langle jB\rangle_{\rm bs} = -Fp_{\rm e}\left\{\frac{L_{31}}{p_{\rm e}}\left[\frac{{\rm d}p_{\rm e}}{{\rm d}\psi}+\frac{{\rm d}p_{\rm i}}{{\rm d}\psi}-\alpha_{\rm i}n_{\rm i}\frac{{\rm d}T_{\rm i}}{{\rm d}\psi}\right]-\frac{L_{32}}{T_{\rm e}}\frac{{\rm d}T_{\rm e}}{{\rm d}\psi}\right\}, \tag{3}$$

*Project supported by the National Natural Science Foundation of China (Grant No 10375018).
†E-mail: shibr@swip.ac.cn

where ψ is the poloidal magnetic flux, $F=RB_{\rm t}$ the poloidal current flux function, and $p_{\rm e(i)}$, $n_{\rm e(i)}$, $T_{\rm e(i)}$ the electron (ion) pressure, density, and temperature, respectively, and

$$\begin{aligned} L_{31} =&[x(0.754+2.21Z+Z^2) \\ &+x^2(0.347+1.24Z+Z^2)]/D_{\rm e}, \\ L_{32} =&x(0.885+2.08Z)/D_{\rm e}, \\ D_{\rm e} =&1.41Z+Z^2+x(0.775+2.65Z+2.0Z^2) \\ &+x^2(0.347+1.24Z+Z^2), \\ \alpha_{\rm i} =&1.17/(1.0+0.46x), \end{aligned} \tag{4}$$

and

$$x=(1.46\sqrt{\varepsilon}+2.4\varepsilon)/(1-\varepsilon)^{3/2}. \tag{5}$$

For the second model[7] that is suitable for a general equilibrium and arbitrary collisional regime,

$$\begin{aligned} \langle jB\rangle_{\rm bs} =&-Fp_{\rm e}\Big\{L_{31}\left[\frac{1}{p_{\rm e}}\frac{{\rm d}p_{\rm e}}{{\rm d}\psi}+\frac{1}{p_{\rm e}}\frac{{\rm d}p_{\rm i}}{{\rm d}\psi}\right] \\ &+L_{32}\frac{1}{T_{\rm e}}\frac{{\rm d}T_{\rm e}}{{\rm d}\psi}+L_{34}\alpha_{\rm i}\frac{p_{\rm i}}{p_{\rm e}}\frac{1}{T_{\rm i}}\frac{{\rm d}T_{\rm i}}{{\rm d}\psi}\Big\}, \end{aligned} \tag{6}$$

where

$$\begin{aligned} L_{31} =&\left(1+\frac{1.4}{1+Z}\right)X_1-\frac{1.9}{1+Z}X_1^2 \\ &+\frac{0.3}{1+Z}X_1^3+\frac{0.2}{1+Z}X_1^4, \end{aligned} \tag{7}$$

$$X_1=\frac{f_{\rm t}}{1+(1-0.1f_{\rm t})\sqrt{\nu_{\rm e*}}+0.5(1-f_{\rm t})\nu_{\rm e*}/Z}, \tag{8}$$

$$L_{32}=L_{32{\rm e}}+L_{32{\rm i}}, \tag{9}$$

$$\begin{aligned} L_{32{\rm e}} =&\frac{0.05+0.62Z}{(1+0.44Z)Z}(X_2-X_2^4) \\ &+\frac{1}{1+0.22Z}[X_2^2-X_2^4-1.2(X_2^3-X_2^4] \\ &+\frac{1.2}{1+0.5Z}X_2^4, \end{aligned} \tag{10}$$

$$\begin{aligned} L_{32{\rm i}} =&-\frac{0.56+1.93Z}{(1+0.44Z)Z}(Y-Y^4) \\ &+\frac{4.95}{1+2.48Z}[Y^2-Y^4-0.55(Y^3-Y^4)] \\ &-\frac{1.2}{1+0.5Z}Y^4, \end{aligned} \tag{11}$$

$$X_2=\frac{f_{\rm t}}{1+0.26(1-f_{\rm t})\sqrt{\nu_{\rm e*}}+0.18(1-0.37f_{\rm t})\nu_{\rm e*}/\sqrt{Z}}, \tag{12}$$

$$Y=\frac{f_{\rm t}}{1+(1+0.6f_{\rm t})\sqrt{\nu_{\rm e*}}+0.85(1-0.37f_{\rm t})\nu_{\rm e*}(1+Z)}, \tag{13}$$

$$\begin{aligned} L_{34} =&(1+\frac{1.4}{1+Z})X_3-\frac{1.9}{1+Z}X_3^2 \\ &+\frac{0.3}{1+Z}X_3^3+\frac{0.2}{1+Z}X_3^4, \end{aligned} \tag{14}$$

$$X_3=\frac{f_{\rm t}}{1+(1-0.1f_{\rm t})\sqrt{\nu_{\rm e*}}+0.5(1-0.5f_{\rm t})\nu_{\rm e*}/Z}, \tag{15}$$

$$\begin{aligned} \alpha_{\rm i} =&\frac{1}{1+0.15\nu_{\rm i*}^2f_{\rm t}^6} \\ &\times\left[\frac{\alpha_0+0.25(1-f_{\rm t}^2)\sqrt{\nu_{\rm i*}}}{1+0.5\sqrt{\nu_{\rm i*}}}+0.315\nu_{\rm i*}^2f_{\rm t}^6\right], \end{aligned} \tag{16}$$

$$\alpha_0=-\frac{1.17(1-f_{\rm t})}{1-0.22f_{\rm t}-0.19f_{\rm t}^2}. \tag{17}$$

In the above expressions, $\nu_{\rm e*}$ and $\nu_{\rm i*}$ are the effective collision frequencies that divide into the collisionless and collisional regimes, and they are defined as

$$\nu_{\rm e*}=6.921\times10^{-18}\frac{qRn_{\rm e}Z\ln\Lambda_{\rm e}}{\varepsilon^{3/2}T_{\rm e}^2}, \tag{18}$$

$$\nu_{\rm i*}=4.9\times10^{-18}\frac{qRn_{\rm i}Z^4\ln\Lambda_{\rm i}}{\varepsilon^{3/2}T_{\rm i}^2}, \tag{19}$$

where $\ln\Lambda_{\rm e}$ and $\ln\Lambda_{\rm i}$ are respectively the well-known Coulomb logarithms for the electrons and ions, q is the safety factor, R the major radius, Z the charge number of an ion. Now we discuss the calculation of the trapped particle fraction $f_{\rm t}$ defined as

$$f_{\rm t}=1-\frac{3}{4}\langle h^2\rangle\int_0^1\frac{\lambda{\rm d}\lambda}{\langle(1-\lambda h)^{1/2}\rangle}, \tag{20}$$

where $h=B/B_{\max}$, B is the magnitude of the local magnetic field, $B_{\max}$ its maximum value on a given magnetic surface. The determination of the total bootstrap current needs to calculate $f_{\rm t}$ as a function of magnetic flux and other equilibrium quantities. The direct calculation of this double-integration appearing in (20) is usually cumbersome and time consuming. Approximate methods now are available and we select one of them[12] as follows:

$$\bar{f}_{\rm t}=0.75f_{\rm tu}+0.25f_{\rm tl}, \tag{21}$$

where $f_{\rm tu}$ and $f_{\rm tl}$ represent the upper and the lower bounds of the $f_{\rm t}$ value, respectively, while these two values can be easily calculated

$$f_{\rm tu}=1-\frac{\langle h^2\rangle}{\langle h\rangle^2}\left[1-(1-\langle h\rangle)^{1/2}\left(1+\frac{\langle h\rangle}{2}\right)\right], \tag{22}$$

$$f_{\rm tl}=1-\langle h^2\rangle\left\langle h^{-2}\left[1-(1-h)^{1/2}\left(1+\frac{h}{2}\right)\right]\right\rangle. \tag{23}$$

It should be noted that the first coefficient L_{31} is positive and generally a monotonically increasing function

of f_t and a decreasing function of ν_{e*}; the second coefficient L_{32} is negative and varies non-monotonically both with f_t and with ν_{e*}.[7] A clear-cut picture of the bootstrap current scaling then is not so easy to be obtained.

3. Equilibrium model

A typical ST configuration is usually obtained by means of numerical codes. Then, for an equilibrium given by a numerical code, we need to perform calculation of the bootstrap current once. If we hope to establish a scaling, it is necessary to do this many times. Now we have to resort to a general method by giving a simple equilibrium, the so-called Solov'ev configuration[13,14] that is frequently used in stability analysis. It should be pointed out that this simple configuration corresponds to a quasi-uniform toroidal current profile while the bootstrap current usually has a hollow profile, so that the alignment of these two profiles is not good. However, the total bootstrap fraction is not a function sensitive to such an alignment. The merit of the Solov'ev configuration is that we can directly calculate relevant magnetic surface averages rather simply for relevant parameters.

So far several modifications of the Solov'ev configuration have been performed.[14–16] The simplest form[17] of the Solov'ev configuration determining the magnetic geometry is described by four free parameters (E, D, ε, R_0) with the cylindrical coordinates R, Z:

$$\psi = \frac{\psi_b}{y_b^2}\left\{\frac{4}{E^2}[1+(1-D)y]\frac{z^2}{R_0^2}+y^2\right\}, \tag{24}$$

where

$$y = \frac{R^2}{R_0^2} - 1. \tag{25}$$

The four parameters are R_0 the major radius of the magnetic axis, E the elongation-related parameter and D the triangular-deformation-related parameter, ε the inverse aspect ratio. At the boundary we have

$$y_b = \frac{2\varepsilon}{1+\varepsilon^2}. \tag{26}$$

Now we introduce a magnetic surface variable y_ψ and poloidal angle-like variable u through the following coordinates transformation:

$$R = R_0\sqrt{1+y_\psi\cos u},$$
$$Z = \frac{ER_0}{2}\frac{y_\psi \sin u}{\sqrt{1+(1-D)y_\psi\cos u}}. \tag{27}$$

The magnetic surface average now becomes

$$\langle A\rangle = \frac{\int_0^\pi \frac{A\,\mathrm{d}u}{\sqrt{1+(1-D)y_\psi\cos u}}}{\int_0^\pi \frac{\mathrm{d}u}{\sqrt{1+(1-D)y_\psi\cos u}}}. \tag{28}$$

A typical configuration for A=1.2, E=3.0, D=–0.014 is shown in Fig.1.

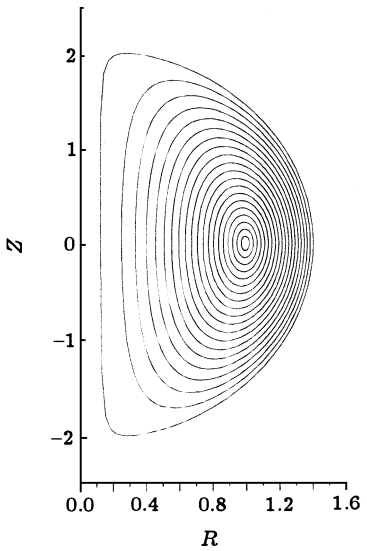


Fig.1. Typical spherical torus configuration with A =1.2, E =3, D=–0.014 and R_0=1.0.

It should be noticed that the elliptic deformation and the triangular deformation of the magnetic surface cross-section are defined respectively as

$$\kappa(\psi) = \frac{S(\psi)}{\pi a^2(\psi)} = \frac{Ey_\psi^2}{\pi(\sqrt{1+y_\psi}-\sqrt{1-y_\psi})}\int_0^1 \mathrm{d}x \times\int_0^\pi \frac{\mathrm{d}u}{\sqrt{(1+y_\psi\cos u)(1+(1-D)y_\psi\cos u)}}, \tag{29}$$

and

$$\delta(\psi) = \frac{\sqrt{1+y_\psi}+\sqrt{1-y_\psi}-2\sqrt{1+y_*}}{\sqrt{1+y_\psi}-\sqrt{1-y_\psi}}. \tag{30}$$

In Eq.(29), $y_\psi = y_b\sqrt{x}$; in Eq.(29),

$$y_* = \sqrt{\left(\frac{1}{1-D}\right)^2 - y_\psi^2} - \frac{1}{1-D}.$$

In the region near the magnetic axis, i.e. for $y_\psi \to 0$, we have $\kappa \to E$ while $\delta \to \frac{(1-D)y_\psi}{2} \to 0$. The general $\kappa(y_\psi)$ and $\delta(y_\psi)$ for an A=1.2 ST configuration is shown in Fig.2.

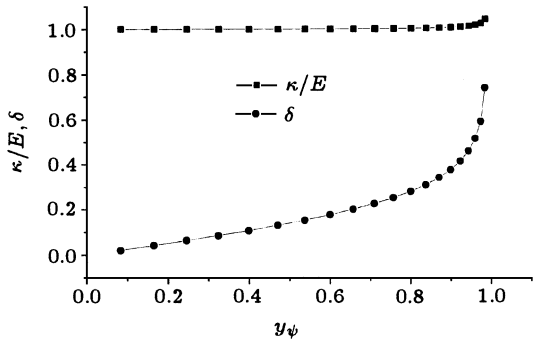


Fig.2. κ/E and δ versus y_ψ for the ST configuration shown in Fig.1.

To calculate the bootstrap current, we still need to know the information about the trapped particle fraction, the plasma density, and the temperature profile. The Solov'ev configuration corresponds to such a pressure profile and a poloidal current profile as

$$p(\psi) = p_0\left(1 - \frac{\psi}{\psi_\mathrm{b}}\right), \tag{31}$$

$$F^2(\psi) = F_0^2 + F_1^2\left(1 - \frac{\psi}{\psi_\mathrm{b}}\right), \tag{32}$$

with

$$p_0 = \frac{8\psi_\mathrm{b}^2}{\mu_0 y_\mathrm{b}^2 E^2 R_0^4}(E^2 + 1 - D), \tag{33}$$

$$F_1^2 = \frac{16D\psi_\mathrm{b}^2}{y_\mathrm{b}^2 E^2 R_0^2}. \tag{34}$$

Now we further assume that the density profile and the temperature profile have the following forms:

$$n_\mathrm{e} = n_{\mathrm{e}0}\left(1 - \frac{\psi}{\psi_\mathrm{b}}\right)^{\alpha_n}, \tag{35}$$

$$T_\mathrm{e} = \tau_\mathrm{e} T_\mathrm{i} = T_{\mathrm{e}0}\left(1 - \frac{\psi}{\psi_\mathrm{b}}\right)^{1-\alpha_n}. \tag{36}$$

Here the ratio of electron temperature to the ion temperature is assumed constant for simplicity. To determine the trapped particle fraction, we need to know the total magnetic field

$$B(y_\psi, u) = \left[\frac{F^2}{R^2} + \frac{(\nabla\psi)^2}{R^2}\right]^{1/2}. \tag{37}$$

From Eq.(24) we obtain the general expression for the poloidal magnetic field $B_\mathrm{p} = |\nabla\psi|/R$ as

$$B_\mathrm{p}(y_\psi, u) = \frac{2\psi_\mathrm{b} y_\psi}{y_\mathrm{b}^2 R_0^2} \times \left\{\left[2\cos u + \frac{(1-D)y_\psi \sin^2 u}{1 + (1-D)y_\psi \cos u}\right]^2 + \frac{4}{E^2}\frac{(1 + (1-D)y_\xi \cos u)\sin^2 u}{1 + y_\psi \cos u}\right\}^{1/2}. \tag{38}$$

To complete the information, we need to set the fifth parameter, i.e. the externally applied toroidal magnetic field $B_{\mathrm{t}0} = F_\mathrm{b}/R_0$. Because for most cases the approximate condition $F \gg |\nabla\psi|$ is satisfied, we mainly discuss this situation. The trapped particle fraction can be easily determined to be independent of the external toroidal magnetic field. Using Eqs.(21)–(23) and (28), we obtain the dependence of the trapped particle fraction on the magnetic surface, as shown in Fig.3. This figure is also applicable to the dependence of the scaling of the largest value of f_t on y_b in different devices. Essentially, this resembles a $\sqrt{\varepsilon}$ scaling. We find that the f_t value is independent of the elongation but only weakly dependent on the triangularity.

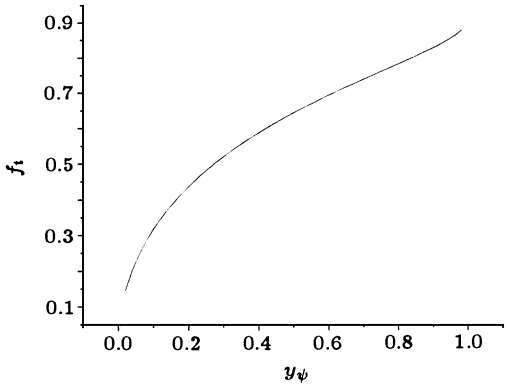


Fig.3. Trapped particle fraction f_t versus y_ψ for A=1.2, D=0. This relation is also true for the maximum f_t versus y_b in different devices.

For the typical ST configuration, the above treatment may induce some errors because the poloidal magnetic field in the region near the edge can be comparable to the toroidal field. To determine the trapped particle fraction in this general case, we need more information about the plasma parameters. However, we find that the difference between the results obtained from this approximate treatment and from the restrict treatment is very small. Only for reference, we write here the restrict h function over any magnetic surface as follows:

$$h = \frac{B}{B_\mathrm{max}} = \frac{1}{\left[1 + \dfrac{E^2(1-y_\psi)y_\psi^2}{4q_0^2}\right]^{1/2}} \times \left[\frac{1 - y_\psi}{1 + y_\psi \cos u} + \frac{E^2(1-y_\psi)y_\psi^2}{4q_0^2} f^2(y_\psi, y)\right]^{1/2} \tag{39}$$

with

$$f = \left\{ \left[\cos u + \frac{1}{2} \frac{(1-D) y_\psi \sin^2 u}{1+(1-D) y_\psi \cos u} \right]^2 + \frac{1}{E^2} \frac{(1+(1-D) y_\psi \cos u) \sin^2 u}{1 + y_\psi \cos u} \right\}^{1/2}. \quad (40)$$

4. Bootstrap current fraction: Model I

For the bootstrap current fraction $f_{\rm bs}$, we first discuss model I. For the Solov'ev configuration, the toroidal current density is

$$j_\zeta(R,\psi) = -R\frac{{\rm d}p}{{\rm d}\psi} - \frac{1}{2\mu_0}\frac{{\rm d}F^2}{{\rm d}\psi}, \quad (41)$$

and the total toroidal current is

$$I_{\rm p} = \frac{4E\psi_{\rm b}}{\mu_0 R_0}\left[\left(1+\frac{1-D}{E^2}\right)I_2 + \frac{D}{E^2}I_3\right], \quad (42)$$

where I_2 and I_3 are integrals respectively defined by

$$I_2(y_{\rm b}, D) = \int_{-1}^{1} {\rm d}u \sqrt{\frac{1-u^2}{1+(1-D)y_{\rm b}u}}, \quad (43)$$

$$I_3(y_{\rm b}, D) = \int_{-1}^{1} \frac{{\rm d}u}{1+y_{\rm b}u}\sqrt{\frac{1-u^2}{1+(1-D)y_{\rm b}u}}. \quad (44)$$

The total bootstrap current can be expressed by

$$I_{\rm bs} = \int_0^{\psi_{\rm b}} {\rm d}\psi \frac{\langle jB\rangle_{\rm bs}}{F}\left\langle \frac{1}{R^2}\right\rangle \oint \frac{{\rm d}l_{\rm p}}{B_{\rm p}} = \frac{ER_0 y_{\rm b}^2}{2}\int_0^1 {\rm d}x \frac{\langle jB\rangle_{\rm bs}}{F} \times \int_0^{\pi} \frac{{\rm d}u}{\sqrt{1+(1-D)y_{\rm b}\sqrt{x}\cos u}}. \quad (45)$$

Now for model I, substituting Eqs.(3)–(5) into the above equation, we obtain

$$I_{\rm bs} = \frac{y_{\rm b}^2 R_0^3 E P_0}{4\psi_{\rm b}}\left\{ \int_0^1 {\rm d}t L_{31} I_0 + \frac{(1-\alpha_n)\tau_{\rm e}}{1+\tau_{\rm e}}\int_0^1 {\rm d}t \alpha_{\rm i} L_{31} I_0 - \frac{(1-\alpha_n)}{1+\tau_{\rm e}}\int_0^1 {\rm d}t L_{32} I_0 \right\}, \quad (46)$$

$$I_0(y_\psi, D) = \int_0^{\pi} \frac{{\rm d}u}{\sqrt{1+(1-D)y_\psi \cos u}}. \quad (47)$$

We note that the relevant integrals in the braces of the right-hand side of Eq.(46) are only functions of the equilibrium quantities; this means that the total bootstrap current is proportional to $P_0/\psi_{\rm b}$. Using (33), we obtain

$$I_{\rm bs} = 0.252 y_{\rm b} R_0 \sqrt{E^2+1-D} \times \sqrt{n_{\rm e0}(T_{\rm i0}+T_{\rm e0})}\, g(\alpha_n, \tau_{\rm e}, y_{\rm b}, D). \quad (48)$$

Here the current is measured in MA, temperature in 10keV, density in $10^{20}{\rm m}^{-3}$. The function g in Eq.(48) expresses the terms appearing in the braces of the right-hand side of Eq.(46). This gives the scaling of the total bootstrap current with respect to the plasma parameters as follows:

$$I_{\rm bs} \propto R_0\sqrt{n_{\rm e0}T_0}. \quad (49)$$

It also depends on the equilibrium quantities: $I_{\rm bs} \propto y_{\rm b}\sqrt{E^2+1-D}\,g$, as shown in Fig.4. It is seen from Eq.(42) that the total toroidal current is also a function of equilibrium quantities. Then, the bootstrap current fraction scaling with respect to the aspect ratio becomes

$$f_{\rm bs} = \frac{g}{2[I_2 + DI_3/(E^2+1-D)]} \quad (50)$$

and it is shown in Fig.5, while in the triangularity case, it is shown in Fig.6 for A=1.4. It seems that the gain of the bootstrap current fraction, resulting from the decrease of the aspect ratio, is not remarkable (slower than the $\sqrt{\varepsilon}$-dependence) and the dependence of the fraction gain on the triangular deformation is also relatively weak.

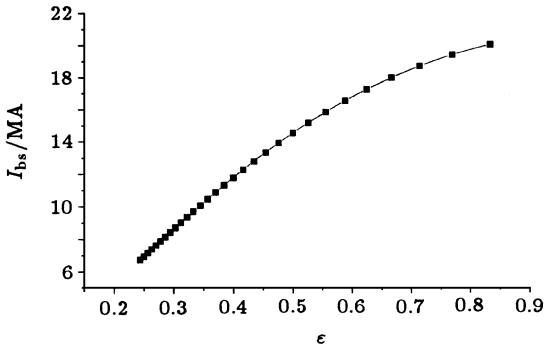


Fig.4. The total bootstrap current versus ε for R_0=4m, $n_{\rm e0}$=1.4, $T_{\rm e0}$=2, $T_{\rm i0}$=1.8.

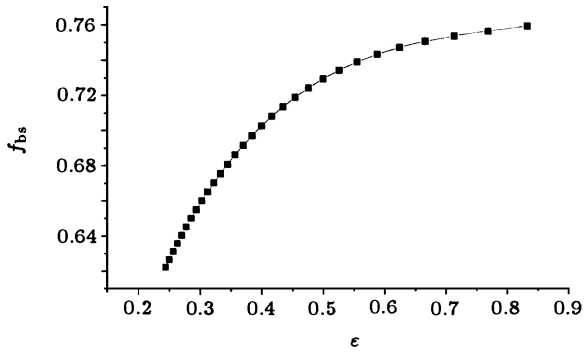


Fig.5. f_{bs} versus ε for $D = 0$.

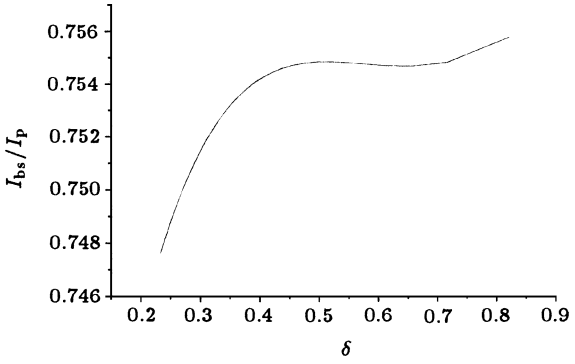


Fig.6. f_{bs} versus δ for A=1.4 for model I.

5. Bootstrap current fraction: model II

To calculate the bootstrap current fraction for model II, it is necessary to set other plasma parameters to complete the definition of a physical equilibrium. Generally, we face different transport regimes for a given equilibrium according to the criteria for the collisional and the collisionless regimes, which are characterized by $\nu_{e,i*} < 1$ (the banana regime), $\nu_{e,i*} \approx 1$ (the plateau regime) and $\nu_{e,i*} > 1$ (the collisional regime) that are in turn determined by the plasma density and the plasma temperature as well as the safety factor q for a given magnetic surface with the inverse aspect ratio ε. The profile of the safety factor q is obtained from its definition and here is expressed by

$$q(y_\psi) = \left(\frac{F}{2\pi}\right)\frac{Ey_b^2}{4\psi_b} \times \int_0^\pi \frac{\mathrm{d}u}{(1+y_\psi\cos u)\sqrt{1+(1-D)y_\psi\cos u}}. \quad (51)$$

Now we consider a D-T burning plasma (Case I) and an experimental plasma (Case II) in an ST-like configuration with the following parameters: in Case I $n_{e0} = 1.4\times10^{20}\mathrm{m}^{-3}$, T_{e0}=20keV, T_{i0}=18keV, R_0=4m and in Case II the density is the same as in Case I but the temperature is lower: T_{e0}=5keV, T_{i0}=4.5keV and the device size is smaller: R_0=1m. The other parameters should be subjected to the recognized operation limits for the magnetic fusion machine, such as the beta limit and the density limit that we do not discuss in detail here. For example, now consider an ST configuration with A=1.4, E=3.0, $D = -0.05$, we can obtain $\psi_b = \frac{y_b E R_0^2}{2}\sqrt{\frac{\mu_0 n_{e0}(T_{e0}+T_{i0})}{2(E^2+1-D)}}$=5.24Wb (Case I); 0.164Wb (Case II) from Eq.(33) and $F_1^2 = -0.17(\mathrm{T.m})^2$ (Case I); –0.04 $(\mathrm{T.m})^2$ (Case II) from Eq.(34). We find that $F_1^2 \ll F_b^2$. The safety factor at the magnetic axis is[16] $q_0 = ER_0y_b^2F/8\psi_b$, this gives B_{t0}/q_0=0.973T. Setting q_0=1.46 yields an external applied toroidal magnetic field B_{t0}=1.5T.

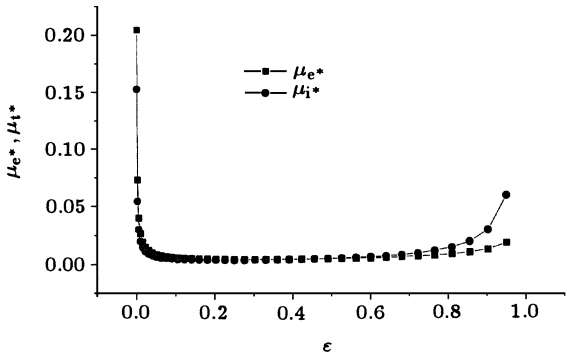


Fig.7. μ_{e*} and μ_{i*} versus ε for Case I.

It can be seen from Figs.7 and 8 that Case I corresponds to a pure banana regime over the whole plasma cross-section while Case II a banana and plateau mixed regime. The total bootstrap current and its fraction can be expressed by expressions similar to Eqs.(45)–(48) but with a much more complicated function g that is a function of not only equilibrium quantities but also plasma parameters through Eqs.(7)–(20). Compared to model I, the more realistic model II gives smaller total bootstrap current and its fraction, and it is also found that this fraction is not sensitive to the variation of the triangularity (Fig.9). The scaling with respect to the inverse aspect ratio is shown in Fig.10 that is slower than the $\sqrt{\varepsilon}$ dependence, the same as in the model I. The absolute bootstrap current in this case is shown in Fig. 11, which shows a remarkable increase of its value with the increase in ε, as expected. Finally, for the experimental Case II, results are similar to those in Case I, but the absolute bootstrap current and its fraction are both smaller than those in the reactor (Case I). They are shown in Figs.12 and 13, respectively.

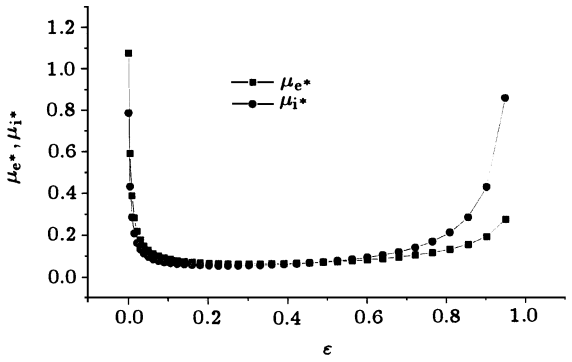


Fig.8. μ_{e*} and μ_{i*} versus ε for Case II.

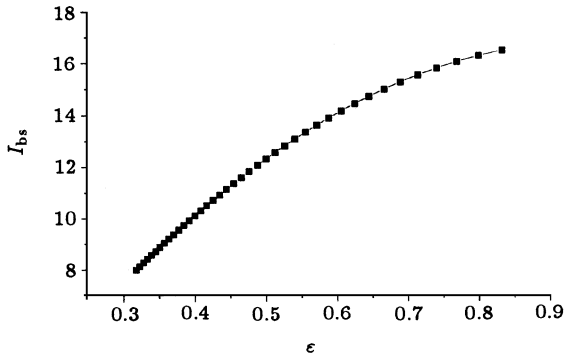


Fig.11. The absolute bootstrap current I_{bs} versus ε as in Fig.10.

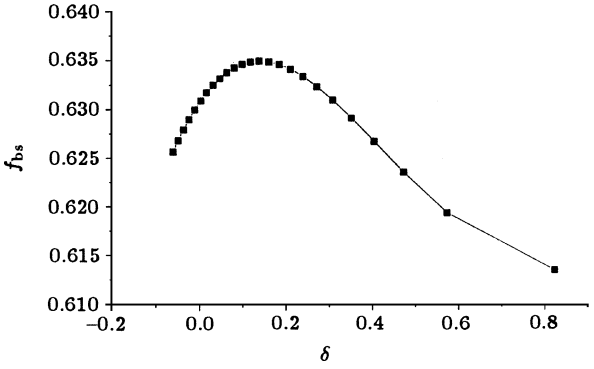


Fig.9. f_{bs} versus δ for A=1.4, q_0=3.0, n_{e0}=1.4, T_{e0}=20keV, T_{i0}=18keV. The absolute value of I_{bs} is about 10.5MA.

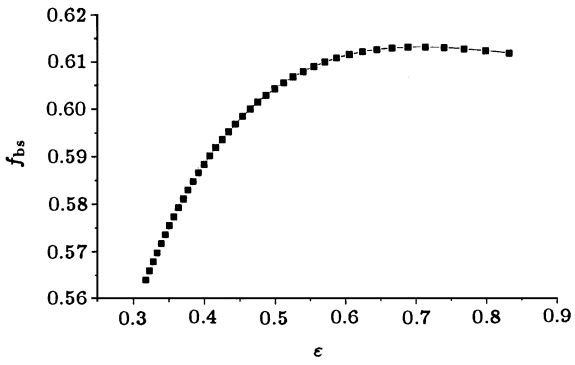


Fig.12. The relation of f_{bs} versus ε is the same as that in Fig.10 for the experimental ST Case II: R_0=1m, T_{e0}=5keV, T_{i0}=4.5keV.

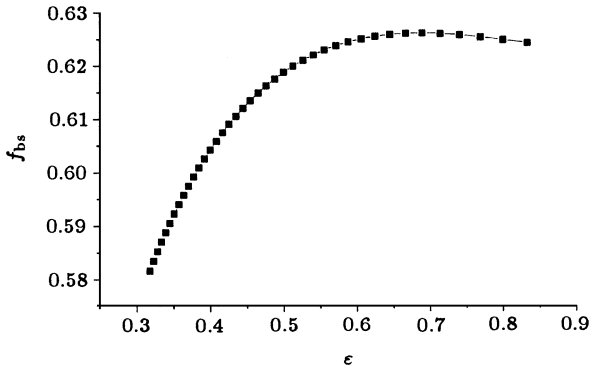


Fig.10. f_{bs} versus ε for q_0=1.5, n_{e0}=1.4, T_{e0}=20keV, T_{i0}=18keV. And D=0.

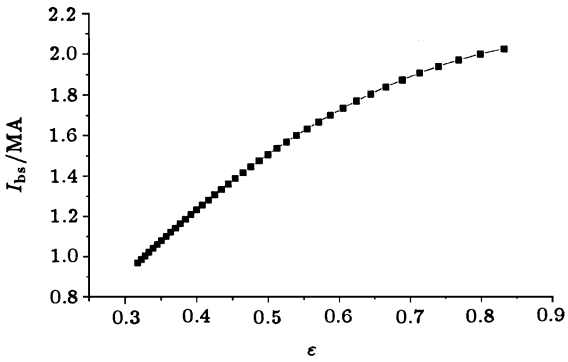


Fig.13. I_{bs} versus ε for Case II as in Fig.12.

6. Summary

We have studied the scaling of the bootstrap current fraction by using two typical models and found that it is not sensitive to the change of the triangularity, which is beneficial for the improvement of the MHD stability. For a given plasma minor radius, the absolute bootstrap current increases with the decrease of the aspect ratio while the bootstrap fraction increases slowly. The more realistic model II gives a smaller value than the collisionless model I even for the case where the plasma is actually in a full banana regime. Because all these results are obtained based on the Solov'ev equilibrium, we need check its universality against the equilibrium configuration in future work.

References

[1] Sykes A 1994 Plasma *Phys. Contr. Fusion* **36** B93
[2] Peng Y K M and Strickler D J 1986 *Nucl. Fusion* **26** 769
[3] Peng Y K M *et al* 2000 *Phys. Plasmas* **7** 1681
[4] Hirshman S P 1988 *Phys. Fluids* **31** 3150
[5] Kessel C E 1994 *Nucl. Fusion* **34** 1221
[6] Peeters A G 2000 *Plasma Phys. Contr. Fusion* **42** B231
[7] Sauter O *et al* 1999 *Phys. Plasma* **6** 2834
Sauter O *et al* 2002 *Phys. Plasmas* **9** 5140
[8] Houlberg W A *et al* 1997 *Phys. Plasmas* **4** 3220
[9] Shaing K C *et al* 1995 *Phys. Plasmas* **2** 349
[10] Shaing K C *et al* 1996 *Phys. Plasmas* **3** 965
[11] Gong X Y *et al* 2002 *Acta Phys. Sin.* **51** 2547 (in Chinese)
[12] Lin-liu Y R and Miller R L 1995 *Phys. Plasmas* **2** 1668
[13] Solov'ev L S 1968 *Soviet Phys. JETP* **26** 400
[14] Zheng S B, Wootton A J and Solano E R 1996 *Phys. Plasmas* **3** 1176
[15] Weening R H 1997 *Phys. Plasmas* **4** 3254
[16] Weening R H 2000*Phys. Plasmas* **7** 3654
[17] Shi B R 2003 *Plasma Sci. Tech.* **5** 1849